JOURNAL OF OPTOELECTRONICS AND ADVANCED MATERIALS Vol. 13, No. 11-12, November – December 2011, p. 1570 - 1576

Molecular dynamics simulation studies on melting of Sn nanowires

S. SENTURK DALGIC*, U. DOMEKELI
Department of Physics, Faculty of Science, University of Trakya, 22030, Edirne

The melting process of Sn nanowires has been simulated by using molecular dynamics with the modified analytic embedded atom method (MAEAM) interatomic potentials. The wires studied here are chosen approximately cylindrical in cross-section. The periodic boundary conditions has been applied along their length; the atoms were arranged initially in a crystal structure of β-Sn block which belongs to tetragonal group with the [0 0 1] direction parallel to the long axis of the wire. The size effects of the nanowires on the melting temperatures have been investigated. In order to characterize melting transition, we have interested in some structural, energetic and dynamical quantities of Sn nanowires. We find that for the nanoscale regime, the melting temperatures of Sn nanowires are much lower than that of the bulk. It has been resulted that melting point of Sn nanowires shifts to higher temperatures when the diameter of nanowires increased. There is in a good agreement between the results obtained from MD simulations and other theoretical and experimental data. When a nanowire is heated up above the melting temperature, the neck of the nanowire begins to arise and the diameter of neck decreases rapidly with the equilibrated running time. Finally, the breaking of nanowire arises, which leads to the formation of the spherical nanoparticles.

(Received June 2, 2011; accepted November 23, 2011)

Keywords: Sn Nanowires, MD simulation, Melting process

1. Introduction

In recent years, the study of nanomaterials is a fascinating area of research. Because of the large fraction of surface atoms in the surface, the physical, chemical, and electronic properties of them are strongly dependent on their size, shape, dimensional and composition [1-3]. As one of the most important one dimensional nanomaterials, nanowires (NWs) have attracted a great deal of interests because of their pivotal role in future electronic, opto-electronic, and nano – electromechanical systems [4]. Meanwhile, metallic NWs are candidate materials for passive interconnects in future nanodevices, therefore, understanding of the size-dependent thermal stability as well as the melting features is a key element to realizing good metallurgical bonding and reliability of NWs interconnects.

Sn NWs have attracted much attention, and a variety of growth methods have been developed. Electrochemical synthesis with a porous template has been used for the growth of NWs [5-9]. Inside the template, the NWs are prevented from oxidation, however, when the template is removed, they are easily oxidized. Ion beam etch process can be adopted for the oxide removal [7]. In electronic devices, Sn and some of its alloys are being used as interconnect materials in on-chip and off-chip applications. Due to their high melting point (~500 K), a high reflow temperature will be needed in the electronics manufacturing process. This high process temperature in electronics assembly has adverse effects not only on energy consumption, but also on substrate warpage, thermal stress and popcorn cracking in molding compounds, resulting in poor reliability of the devices. Therefore studies on lowering processing temperature of Sn are being paid attention [10]. As we know, for crystals the structure is an important determinant to their melting process which starts from the surface layer and propagates into the interior; the melting temperature of surface is significantly lower than that of the bulk [11,12]. The melting behavior of Sn NWs have exhibited dramatically different character from their bulk counterpart both experimentally and theoretically [9,13,14]. Shin et al. [9] studied thermal instability and melting behavior of Sn NWs by differential scanning calorimetry. The melting temperature of NWs has been investigated extensively by many outstanding theoretical models. Li et al. [14] reported the size – dependent melting temperature of Sn NWs using a theoretical model. Surface atoms have fewer nearest neighbors and weaker bonding which could lead to an earlier surface melting behavior [15,16]. It has been established experimentally that the melting begins preferentially at the surface in the melting process of nanoparticles and nanowires [17,18]. Qi et al. [19] reports that the melting proceeds from the surface inwards, and the mesoscale regime is characterized by the surface melting. It is therefore to be expected that the melting temperature of a nanowire decreases with the reduced diameter size, because the fraction of the atoms that resides in or near a surface increases drastically. However, the molecular dynamics (MD) studies for the helical multi-walled cylindrical gold NWs by Wang et al. [20] demonstrate that the melting process starts from the interior region; the surface melting happens at relatively higher temperatures. They argue that the surface melting

represents the overall melting in ultrathin metallic NWs. Therefore, it is also important to study and compare the melting behaviors for different materials under different configurations. Since metal NWs have a number of exciting potential applications in nanoscale electronic devices, it is necessary to develop a quantitative understanding of the thermodynamic and structural properties of such metal NWs. Computer simulation at the atomic level provides a useful tool to analyze structural, mechanical and thermodynamic properties of nanomaterials, and eventually to design materials of assigned characteristics. MD simulation, as one of the most important methods of atomistic simulations, may display the phase-space trajectories of particles through the solution of Newton's equation, thereby shedding light on how atomic level processes can lead to macroscopic phenomena, and provides a useful complement to experimental studies based on STM or AFM. MD simulations have already been employed to study the structures and properties of free-standing metal NWs [11,17-24].

In the present study, we report the melting process of Sn NWs using molecular dynamics simulations with modified analytic embedded atom method (MAEAM) [25-28] which was applied to nanoparticles in our previous works [27,28]. The MD simulation code of DLPOLY is used in our calculations [29]. We also present the size effect on the overall melting process of the Sn NWs. Even though it can be of particular interest, the melting process of Sn NWs has not yet been studied by MD simulations to our knowledge.

2. Computational method

2.1 Modified analytic embedded atom method

In the MAEAM model, the total energy of a system E_{tot} can be written as [26]

$$E_{tot} = \frac{1}{2}\sum_i \sum_{j\neq i} \phi(r_{ij}) + \sum_i F(\rho_i) + \sum_i M(P_i) \tag{1}$$

$$\rho_i = \sum_{j\neq i} f(r_{ij}) \tag{2}$$

$$P_i = \sum_{j\neq i} f^2(r_{ij}) \tag{3}$$

where $\phi(r_{ij})$ the pair potential between atoms i and j, r_{ij} is the separation distance of atom j from atom i, $F(\rho_i)$ is the energy to embed an atom in site i with electron density ρ_i which is given by a linear superposition of spherical averaged atomic electron density of other atoms $f(r_{ij})$ and $M(P_i)$ the modified term, which describes the energy change due to nonspherical distribution of atomic electronic density and deviation from the linear superposition. Pair potential $\phi(r_{ij})$, embedding function $F(\rho_i)$, modified term $M(P_i)$, and atomic electron density $f(r_{ij})$ take the following forms [26-28]:

$$\phi(r_{ij}) = k_0 + k_1\left(\frac{r_{ij}}{r_{1e}}\right)^2 + k_2\left(\frac{r_{ij}}{r_{1e}}\right)^4 + k_3\left(\frac{r_{1e}}{r_{ij}}\right)^{12} \tag{4}$$

$$F(\rho_i) = -F_0\left[1 - n\ln\left(\frac{\rho_i}{\rho_e}\right)\right]\left(\frac{\rho_i}{\rho_e}\right)^n \tag{5}$$

$$M(P_i) = \alpha\left\{1 - \exp\left[-10000.0\left(\ln\left(\frac{P_i}{P_e}\right)\right)^2\right]\right\} \tag{6}$$

$$f(r_{ij}) = f_e\left(\frac{r_{1e}}{r_{ij}}\right)^6 \tag{7}$$

where subscript e indicates equilibrium and r_{1e} is the first-neighbor distance in the equilibrium state. The electron density at equilibrium state f_e is chosen as [27]

$$f_e = \left(\frac{E_c - E_{1v}^f}{\Omega}\right)^{3/5} \tag{8}$$

where Ω is the atomic volume. The model parameters k_0, k_1, k_2, k_3, F_0, n and α are determined by fitting the physical properties of tin, such as cohesive energy, vacancy formation energy, lattice parameter and elastic constants. In this model, the two-body potential and the electron density functions should be cut off. A cubic spline function is used as a cutoff function. The cutoff procedure is the same as that used by Zhang et al. [25] with the start point r_s=r_2 and the end point r_c = 0.86a_0, where r_2 is the second-neighbor distance.

2. 2 Simulation procedure

In order to simulate the melting processes of Sn NWs and to investigate the size effects of NWs on melting temperature, we constructed eight NWs consisting of 1776, 2736, 3888, 5808, 8496, 14448, 24816 and 35952 atoms, representing the diameter of NWs ranging from 1.85 to 9.0nm. All NWs are extracted from a large the crystal structure of β-Sn block which belongs to tetragonal group ($25a_0$ x $25a_0$ x $50c$) using various cylindrical cutoff radii centered at a cubic interstitial site, in which the crystallographic orientations in the *X*-, *Y*-, and *Z*-axis are taken to be in the direction of [100], [010] and [001], respectively. In the *X* and *Y* directions the Sn NWs constructed a finite number of unit cells, while in the *Z*-direction an infinite wire was obtained by applying the periodic boundary conditions. The length of NWs adopt in the MD simulation is initially 15.8nm (50 unit cells in Z direction). In order to get an energy-optimized structure during heating at a given temperature for the bulk systems

it is performed molecular dynamics under constant temperature and constant pressure condition (NPT) with a periodic boundary conditions. For the NWs, we used the constant volume and constant temperature (NVT) molecular dynamic simulations. At as a first step, both bulk and nanowire have been stabilized by relaxing for 50ps at 286 K given conditions. For each NWs, the system undergoes the heating process consisting of a series of MD simulations with the temperature increment of ΔT=10 K. The simulations are carried out for 50ps to relax the nanowire system at each temperature. The Newtonian equations of motion are integrated using the Leapfrog Verlet method with a time step of 2.5 fs. The desired temperature and ambient pressure are controlled by Nose-Hoover thermostat [30,31] and Berendsen approach [32], respectively in conjunction with DLPOLY simulation code [29].

2. 3 The structure and dynamics properties

The radial distribution function of $g(r)$ is regarded as one of the most parameters that are used to describe the structure characterization of solid, amorphous and liquid states. It is defined as:

$$g(r) = \frac{\Omega}{N^2}\left\langle \left(\sum_{i=1}^{N_i} n_i \right) / 4\pi r^2 \Delta r \right\rangle \tag{9}$$

where, $g(r)$ is the probability of finding an atom in a distance ranging from r to $r+\Delta r$. Ω is simulated volume of unit cell. N is the Number of atoms in the systems, and N_i is the averaged number atom around ith atoms sphere shell ranging r to $r+\Delta r$, where Δr is the step of calculation. The diffusion coefficients of the atoms was calculated by using the Einstein equation,

$$D = \lim_{t\to\infty} \frac{\left\langle \Delta r(t)^2 \right\rangle}{6t} \tag{10}$$

where t is the diffusion time, $\left\langle \Delta r(t)^2 \right\rangle$ is the mean square displacement. $\left\langle \Delta r(t)^2 \right\rangle$ of the particle in the MD can be described as:

$$\left\langle \Delta r(t)^2 \right\rangle = \frac{1}{N}\sum_{i=1}^{N} \left| r_i(t+t_o) - r_i(t_o) \right|^2 \tag{11}$$

where $r_i(t_o)$ is the position vector of the ith particle for the system in its initial configuration and $r_i(t)$ is the position vector of ith particle at time t.

3. Result and discussion

To characterize the atomic interactions of Sn, we use the modified analytic embedded atom method, developed by Hu et al. [26]. The MAEAM model parameters for Sn are determined by fitting the physical properties such as cohesive energy, elastic constant, vacancy formation energy and lattice parameter as published our previous work [27]. The calculated MAEAM model parameters for Sn are listed in Table 1. In order to validate the MAEAM potential, we firstly simulate the melting process of bulk Sn and check our results with those presented in the literature.

In this study, we chose the β-Sn phase as a crystal structure because the β-Sn phase, one of two allotropes of Sn, is metallic and stable at temperatures above 286 K to the melting point of 505 K. The equilibrium physical properties at 286K and thermal properties such as melting point, heat of fusion of bulk β-Sn which are obtained by MAEAM potential and compared with experimental [33] and Baskes' s MEAM results [34] listed in Table 2. The physical quantities obtained in this study, are consistent with the values in literature.

Table 2. Comparisons of the calculated properties, lattice constants, cohesive energy, melting point and heat of fusion.

Quantity	MAEAM	Expt[a].	MEAM[b]
a (A)	5.81	5.83	5.92
c (A)	3.17	3.18	3.23
c/a	0.546	0.546	0.546
E_c (eV)	-2.65	-3.10	-3.08
T_m (K)	500	505	453
H_m (kJ/mol)	6.81	7.04	3.09

[a]Ref [33] and [b]Ref [34]

We now discuss our MD simulations on the melting processes of the Sn NWs. In order to work the size effect of the NWs on their melting points, we have simulated the of Sn NWs during heating process with eight different diameters as mentioned in the previous section. The temperature dependences of the mean atomic energy of these NWs are shown in Fig. 1.

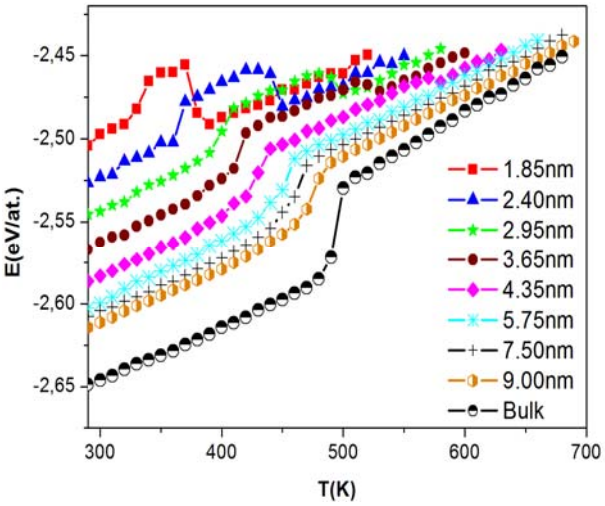

Fig. 1. The mean atomic energy as a function of temperature.

It can be seen that the mean atomic energy for NWs are higher than that of the bulk due to their surface energies, and the exceeded value of nanowire to the bulk increases as the diameter of the nanowire is reduced.

Table 1. The MAEAM model parameters for Sn.

Metal	F_o(eV)	n	α (eV)	f_e(eV/A^3)	k_o(eV)	k_1(eV)	k_2(eV)	k_3(eV)
Sn	1.7900	0.28880	0.00904	0.19628	-0.43194	0.18207	0.00035	0.06057

The average atomic energies of these systems increase approximately linearly with the increasing temperature, except near melting point regime. The typical signature of melting obtained from the caloric curves is a jump in energy. It is obviously seen in Fig. 1 that there is no unique temperature corresponding to the melting transition on the caloric curves. The midpoint of a jump was selected as the melting point in the present work. The mean atomic energy reaches its maximum at the melting point, and then decreases sharply with the further increase of temperature. The reason of an abruptly reduced the mean atomic energy is because of the breaking of the Sn nanowire and the formation of spherical nanoparticles. The size (diameters) dependence of the melting point of Sn-NWs is illustrated in Fig. 2 along with experimental data and those obtained by theoretical model. Clearly, the overall melting points of NWs are much lower value than that of bulk Sn. Thus, it is noted that the diameter of NW decreases melting temperature decreases correspondingly. The depression of the melting temperature is dramatic in the lower range of diameter of NW, while it becomes smoothly in large diameter of NW. Our results are in good agreement with the predictions from both the theoretical [14] and experimental results [9,13].

In Fig. 3, in order to visualize the structure evolution process and to understand the melting behavior of Sn NWs, we recorded the trajectories of atomic motions at various temperatures and times and plotted selectively the snapshots of the melting procedure of NW with the diameter of D=4.35nm. Fig. 3(a) shows the NW maintaining at the initial β-Sn structure. With the temperature of the system increased up to 370 K, the surface atoms of the NWs begin to deviate from their initial positions and a considerable disorder of some surface regions are observed during the equilibrated relaxation in Fig. 3(b).

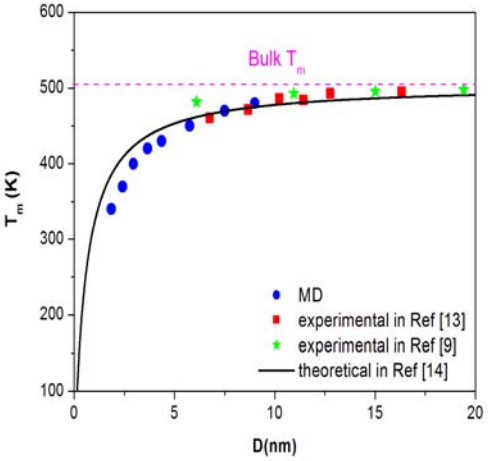

Fig. 2. The melting temperature as a functional of the diameter of Sn nanowire.

From the caloric curves for nanowire with the diameter of D=4.35nm, it can be seen that the overall melting is accomplished at the temperature of 440 K, which is a well-defined melting point. The neck is firstly formed in the nanowire with the diameter of D=4.35nm at around 550 K and is relatively unstable during the relaxation. As the temperature is increased to 570 K disordered necks of decreasing diameters are seen as displayed in Fig. 3(e) and 3(f).

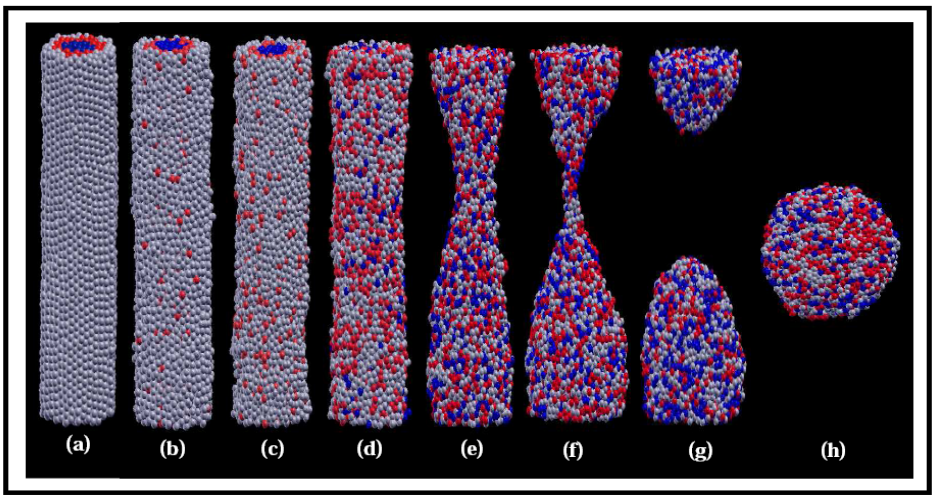

Fig. 3. (a)–(h). MD simulation snapshots of the nanowire with the diameter of D=4.35nm at various temperatures and times in the heating process. (a) 300 K (100 ps), (b) 370 K (100 ps), (c) 410 K (100 ps), (d) 440 K (100 ps), (e) 550 K(100 ps), (f) 570 K (75 ps), (g) 570 K (100 ps), (h) 590 K (100 ps). Note that the number in the parentheses is the relaxed time of MD simulation at the corresponding temperature that the periodic boundary condition in the axes of nanowire is applied.

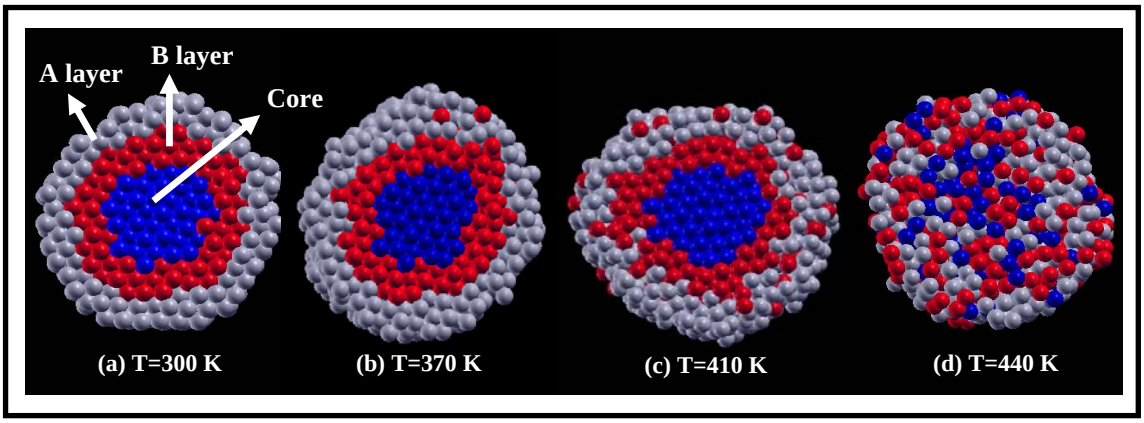

Fig. 4. The X–Y sections of the same Z coordinate for nanowire with the diameter of D=4.35nm at various temperatures and times in the heating process.

In subsequent equilibration at the same temperature, the breaking of the nanowire can be seen in Fig. 3(g). The spherical nanoparticles is finally formed by running a 100 ps at 590 K as shown in Fig. 3(h).

In order to investigate the melting evolution and distinctive surface properties, two cylindrical layer regions with the same thickness of a_0 are divided and labeled as A layer and B layer, starting from the outmost layer, and the remaining is labeled as core (as shown in Fig. 4).

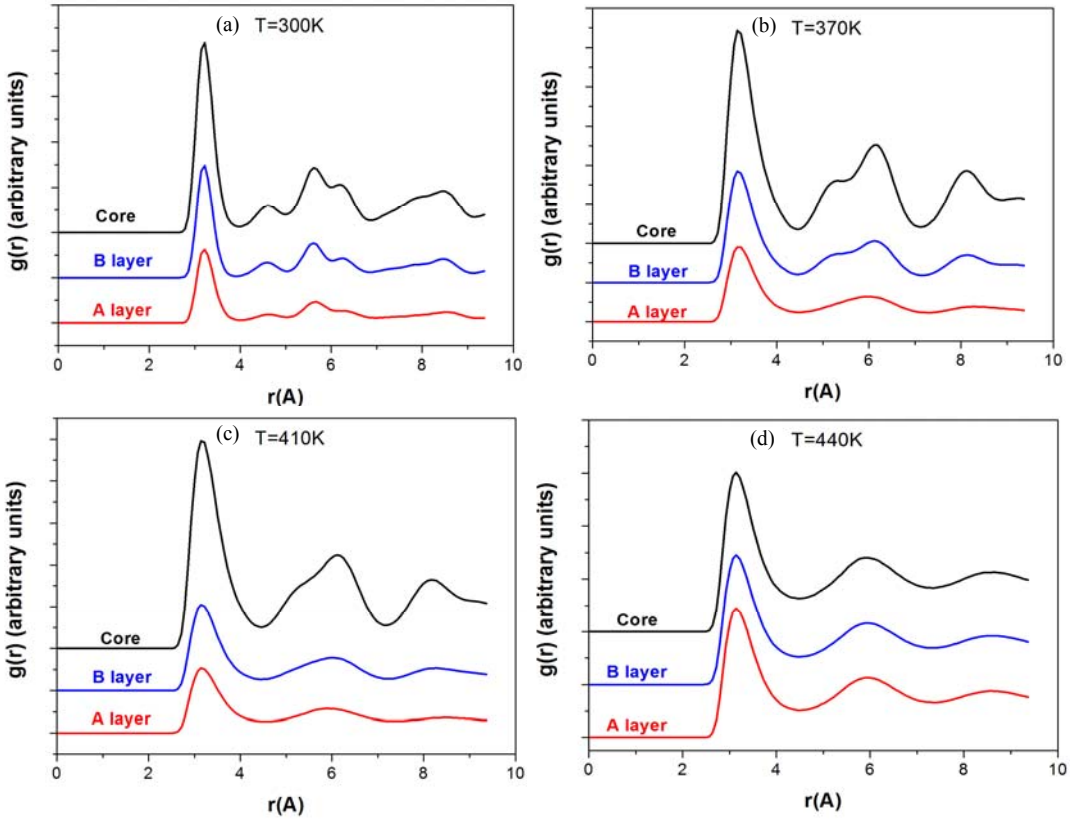

Fig. 5. The radial distribution functions (RDF) of nanowire with the diameter of D=4.35nm at different temperatures.

Fig. 4 displays the atoms on the X – Y cross sections at the same Z position at several typical temperatures during heating, showing a clear picture of the spreading disorder from the A layer to the core, which means that the melting evolution starts from the surface to interior.

The melting evolution between layers has been determined from the calculated structural and dynamical properties of the system which characterizes the structural order and microscopic atomic motion of the system. The structures of the simulated cylindrical Sn NWs are discussed in terms of the g(r). Using the atomic

coordinates, MD predictions of $g(r)$ corresponds to the NW with the diameter of D=4.35nm has been calculated at different temperatures as shown in Fig. 5, at a temperature of 370 K, the RDF of the outmost layer, labeled as A layer, begins to approach the character of the liquid structure, local disordered regions appear on the surface layer, and B layer begins to incline to liquid disorder (as shown in Fig. 4 (b) and Fig. 5 (b)). As the temperature increases to 410 K, B layer turns into liquid and core region begins to lose its ordered structure, (as shown in Fig. 4 (c) and Fig. 5 (c)). After the temperature increases to 440 K, all of the outer layers and the core behave as though fully disordered (as shown in Fig. 4 (d) and Fig. 5 (d). The evolution of atomic configurations with temperature indicates that the premelting on the surface layers is a step-by-step process from the outmost surface. When the temperature approaches the melting point, the core melts suddenly, just as in the conventional crystalline. In Fig. 6, we have plotted the temperature evaluation of the diffusion coefficients for the nanowire with the diameter of D=4.35nm.

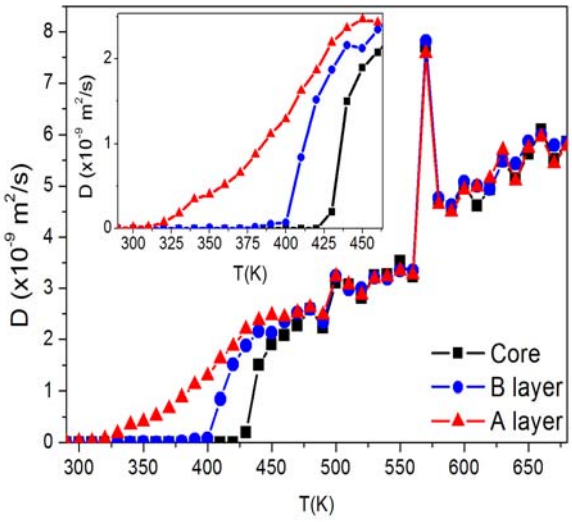

Fig. 6. Temperature dependence of the diffusion coefficient for nanowire with the diameter of D=4.35nm.

As shown in Fig. 6, the diffusion is mainly localized to the surface layers at low temperature, and the diffusion coefficient increases rapidly with increasing temperature. Consisting with the above discussions, the atoms on the surface layers have a very high diffusion coefficient. When the temperature approaches melting point, there is a sudden increase in the diffusion coefficient for all of the layer. Furthermore, even above the melting temperature, the outer layer has higher diffusion coefficients than that of core. B layer exhibits a similar diffusion behavior. Also in this figure, we observed that the value of 570K which corresponds to the temperature of nanowire is broken and diffusion abruptly increases. This situation corresponds to the movement of atoms, very fast toward the periodicity of the simulation box.

4. Conclusions

In this paper, the melting process of Sn NWs have investigated by the molecular dynamics simulation using modified analytic embedded atom method. We show that the overall melting temperatures of Sn NWs are much lower than that of bulk Sn in the nanoscale regime. It has been recognized that there is a relation between diameter of nanowire and melting temperature as well diameter of nanowire decreases melting temperature decreases correspondingly. The obtained results for Sn-NWs are in good agreement with experimental data and the theoretical predictions. When the NWs were heated up above the melting temperature, the neck of a nanowire began to arise and the diameter of the neck decreased rapidly with the equilibrated running time. Finally, the breaking of nanowires happened leading to the formation of spherical nanoparticles. Also in this study, we observed the evolution of atomic configurations with temperature indicates that the premelting on the surface layers is a step-by-step process from the outmost surface. When the temperature approaches the melting point, the core melts suddenly.

References

[1] R. Narayanan, M. A. El-Sayed, J. Phys. Chem. B **109**, 12663 (2005).
[2] C. W. Hills, N. H. Mack, R. G. Nuzzo, J. Phys. Chem. B **107**, 2626 (2003).
[3] H. Bonnemann and R. M. Richards, Eur. J. Inorg. Chem. **10**, 2455 (2001).
[4] S. Iijima, L. C. Qin, B. H. Hong, S. C. Bae, S. Y. Youn, K. S. Kim, Science **296**, 611 (2002).
[5] M. Tian, J. Wang, J. Snyder, J. Kurtz, Y. Liu, P. Schiffer, T. E. Mallouk, M.H.W. Chen, Appl. Phys. Lett. **83**, 1620 (2003).
[6] S. Michotte, S. Matefi-Tempfli, L. Piraux, Appl. Phys. Lett. **82**, 4119 (2003).
[7] D. Lucot, F. Pierre, D. Mailly, K. Yu-Zhang, S. Michotte, F. de M. de Horne, L. Piraux, Appl. Phys. Lett. **91**, 042502 (2007).
[8] T. Djenizian, I. Hanzu, Y. D. Premchand, F. Vacandio, P. Knauth, Nanotechnology **19**, 205601 (2008).
[9] H. S. Shin, J. Yu, J. Y. Song, Appl. Phys. Lett. **91**, 173106 (2007).
[10] H. Jiang, K. Moon, H. Dong, F. Hu, C. P. Wong, Chem. Phys. Lett. **429**, 492 (2006).
[11] O. Gulseren, F. Ercolessi, E. Tosatti, Phys. Rev. B **51**, 7377 (1995).
[12] J. Hu, T. W. Odom, C. M. Lieber, Acc. Chem. Res. **32**, 435 (1999).
[13] M. Zhao, X. H. Zhou, Q. Jiang, J. Mater. Res. **16**, 11 (2001).

[14] Y. J. Li, W. H. Qi, B. Y. Huang, M. P. Wang, S. Y. Xiong, Modern Phys. Lett. B **24**, 2345 (2010).
[15] Z. Liu, et al., Angew. Chem. Int. Ed. Engl. **39**, 3107 (2000).
[16] Y. Xia, et al., Adv. Mater. 15, 353 (2003).
[17] Z. L. Wang, et al., Phys. Rev. B **67**, 193403 (2003).
[18] S. Link, et al., J. Phys. Chem. B **104**, 7867 (2000).
[19] Y. Qi, T. Cagin, W. L. Johnson, W. A. Goddard, J. Chem. Phys. **115**, 385 (2001).
[20] J. Wang, X. Chen, G. Wang, B. Wang, W. Lu, J. Zhao, Phys. Rev. B **66**, 085408 (2002).
[21] B. L. Wang, S. Y. Yin, et al., Phys. Rev. Lett. **86**, 2046 (2001).
[22] H. Ikeda, et al., Phys. Rev. Lett. **82**, 2900 (1999).
[23] P. S. Brancio, J. P. Rino, Phys. Rev. B **62**, 16950 (2000).
[24] Y. H. Wen, Z. Z. Zhu, R. Zhu, G. F. Shao, Physica E **25**, 47 (2004).
[25] B. W. Zhang, Y. F. Ouyang, Phys. Rev. B **48**, 3022 (1993).
[26] W. Y. Hu, B. W. Zhang, X. L. Shu, B. Y. Huang, J. Alloys Compounds **289**, 159 (1999).
[27] S. S. Dalgic, U. Domekeli, J. Optoelectron. Adv. Mater. **11**, 2126 (2009).
[28] S. S. Dalgic, J. Optoelectron. Adv. Mater. **11**, 2133 (2009).
[29] DL_POLY: a molecular dynamics simulation package written by W. Smith, T. R. Forester, I. T. Todorov has been obtained from the website http://www.ccp5.ac.uk/DL_POLY
[30] S. Nose, J. Chem. Phys. **81**, 511 (1984).
[31] W. Hoover, Phys. Rev. A 31, 1695 (1985).
[32] H. J. C. Berendsen, J. P. M. Postma, W. F. van Gunsteren, A. DiNola, J. R. Haak, J. Chem. Phys. **81**, 3684 (1984).
[33] J. Ihm, M. L. Cohen, Phys. Rev. B **23**, 1579 (1981).
[34] R. Ravelo, M. I. Baskes, Phys. Rev. Lett. **79**, 2482 (1997).

* Corresponding author: serapd@trakya.edu.tr